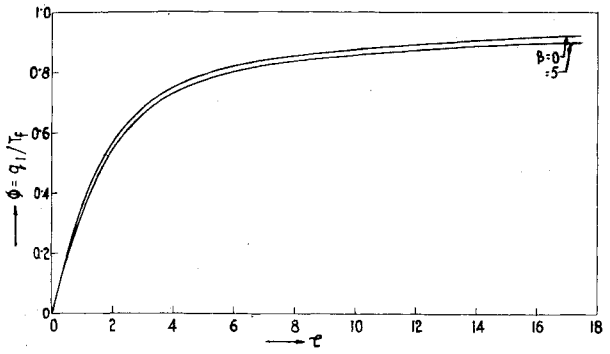

Fig. 1 Variation of surface temperature with time.

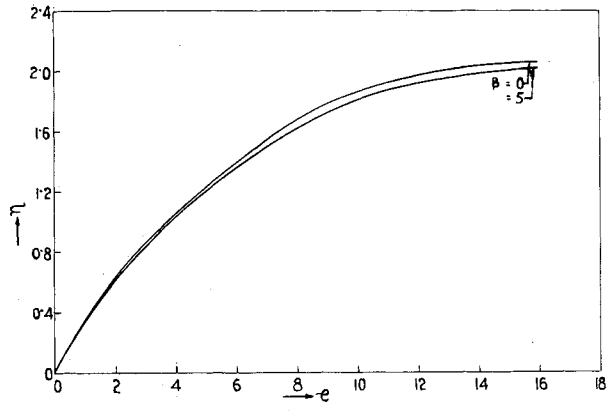

Fig. 2 Variation of melting distance with time.

For the melting solid having very high latent heat ($L\to\infty$), β is zero, and the Eq. (24) becomes

$$\dot{\phi}[3(1-\phi^4)+12\phi^3/(1-\phi^4)^3]=1 \qquad (26)$$

and its solution is

$$\tau=3\phi/(1+\phi^2)+(9/8)\tan^{-1}\phi-(3/8)(1-\phi^2)^{-1}$$
$$+(9/16)\ln(1+\phi)/(1-\phi)+(3/2)(1-\phi^4)^{-2}-(9/8) \qquad (27)$$

Equation (24) can also be written as

$$\tau=\int_0^1[(B_1+B_2\phi+B_3\phi^2)/(A+B\phi)(1-\phi^4)^2$$
$$+(B_4\phi^3+B_5\phi^4+B_6\phi^5)/(A+B\phi)(1-\phi_4)^3]d\phi \qquad (28)$$

To obtain the solution, Eq. (28) is integrated numerically using Simpson's rule. The limit of integration, which varies from 0 to 1, is divided into 100 equal parts, each part being equal to 0.01. This has yielded accurate results. The surface temperature time history $\phi(\tau)$, and the melting distance time history, $\eta(\tau)$, are plotted in Figs. 1 and 2, respectively, for different values of β. It is found that for any β, both the surface temperature and melting distance increase with increase in time and that they decrease at any time with increase in β. This type of behavior also was obtained in aerodynamic ablation.[6]

Conclusion

Biot's variational method has been applied successfully in obtaining the closed-form solution for the phase-change problem with radiative heating. A study of the combined effect of radiative heating and aerodynamic heating on the ablation of melting solids is in progress.

References

[1] Lardner, T.J., "Approximate Solutions to Phase-Change Problems," *AIAA Journal*, Vol. 5, Nov. 1967, pp. 2079-2080.

[2] Biot, M.A. and Daughaday, H., "Variational Analysis of Ablation," *Journal of the Aerospace Science*, Vol. 29, Feb. 1962, pp. 227-229.

[3] Biot, M.A. and Agrawal, H.C., "Variational Analysis of Ablation for Variable Properties," *Transactions of the ASME. Sec. C, Journal of Heat Transfer*, Vol. 86, Aug. 1964, pp. 437-442.

[4] Prasad, A., "Biot's Variational Principle in a Phase-Change Problem," M.S. thesis, Oct. 1968, Dept. Mech. Eng., I.I.T. Kanpur, India.

[5] Prasad, A. and Agrawal, H.C., "Biot's Variational Principle for a Stefan Problem," *AIAA Journal*, Vol. 10, March 1972, pp. 325-327.

[6] Prasad, A. and Agrawal, H.C., "Biot's Variational Principle for Aerodynamic Ablation of Melting Solids," *AIAA Journal*, Vol. 12, Feb. 1974, pp. 250-252.

[7] Goodman, T.R., "The Heat Balance Integral and Its Application to Problems Involving a Change of Phase," *Transactions of the ASME*, Vol. 80, Feb. 1958, pp. 335-342.

Laminar Boundary-Layer Analyses for Parallel Streams with Interfacial Mass Transfer

C. K. Law*
Northwestern University, Evanston, Ill.

Introduction

RECENT studies[1-4] on transient droplet vaporization have stressed the importance of internal circulation on the vaporization characteristics through its effects on heat and mass transport rates within the droplet. This is because, although diffusional transports are always present during any transient, their rates are either much slower than, or at most comparable with, the droplet surface regression rate.[2,5] However, in the presence of internal circulation these transport rates are significantly enhanced such that, in extreme cases, even perpetual uniformity can be maintained within the droplet.[2,6] Hence an understanding of the generation and the intensity of internal circulation is an essential step toward a detailed analysis of the transient droplet vaporization problem.

An important mechanism that generates internal circulation is the shear stress induced at the nonrigid droplet surface by an external gas stream. When the relative velocity between the droplet and the gas stream is high, as is typical near the fuel spray injection port in certain power plants, it has been estimated[4] that both the liquid- and gas-phase Reynolds numbers are sufficiently large to permit the boundary-layer development on both sides of the interface. Whereas a detailed boundary-layer analysis across the interface of the droplet is obviously difficult, an estimate for the amount of induced liquid-phase motion can be obtained by approximating the shoulder region of the droplet as a flat surface.

Lock[7] analyzed the boundary-layer velocity distribution between two parallel streams, with dissimilar freestream velocities and fluid properties, in the absence of interfacial

Received Jan. 14, 1976; revision received June 16, 1976. This work has been sponsored by the National Science Foundation Grant NSF-RANN AER75-09538.

Index categories: Boundary Layers and Convective Heat Transfer—Laminar; Multiphase Flows; Combustion in Heterogeneous Media.

*Associate Professor, Department of Mechanical Engineering and Astronautical Sciences. Member AIAA.

mass transfer. Both Blasius and momentum-integral solutions were obtained.

In the present problem, the processes of vaporization and condensation, respectively, constitute mass being blown into, or sucked from, the gas stream. This interfacial mass transfer is expected to significantly influence the interfacial shear, and subsequently the liquid motion generated. Law and Sirignano,[3] and Law et al.[4] solved this problem using the Blasius analysis. In the present Note, we present the momentum-integral solution to this problem and show that good agreement with the more accurate Blasius solution exists over the entire range of suction as well as when the blowing rate is not too high.

Analyses

The problem analyzed is the two-dimensional motion of two parallel, adjacent streams of incompressible fluid, which are designated by subscripts 1 and 2 and each of which is characterized by its velocity U, density ρ, and viscosity μ. For conceptual convenience, we shall denote streams 1 and 2 as gas and liquid, respectively, and hence the terms "blowing" and "suction," respectively, imply mass addition to and abstraction from the gas. The x axis is parallel to the freestream motion and the positive y axis is directed into the gas. The corresponding x and y velocity components are u and v, respectively.

The requirement of no slip necessitates the existence of viscous layers on each side of the interface, through which mass and momentum exchange between the two streams takes place. The boundary-layer equations are

Continuity:
$$\frac{\partial u}{\partial x}+\frac{\partial v}{\partial y}=0 \tag{1}$$

Momentum:
$$u\frac{\partial u}{\partial x}+v\frac{\partial u}{\partial y}=\nu_1\frac{\partial^2 u}{\partial y^2} \qquad y>0 \tag{2}$$

$$u\frac{\partial u}{\partial x}+v\frac{\partial u}{\partial y}=\nu_2\frac{\partial^2 u}{\partial y^2} \qquad y<0 \tag{3}$$

The boundary conditions are that at the freestreams $u\to U_1$ and U_2. Across the interface, the requirements of no velocity slip, continuity of horizontal shear, and continuity of normal mass flux are given, respectively, by

$$u_{0+}=u_{0-} \tag{4}$$

$$\mu_1(\partial u/\partial y)_{0+}=\mu_2(\partial u/\partial y)_{0-} \tag{5}$$

$$\rho_1 v_{0+}=\rho_2 v_{0-} \tag{6}$$

In the following, we first present the detailed momentum-integral analysis and then a summary of the Blasius analysis for the previous set of equations.

Momentum-Integral Analysis

We first consider the solution for the gas stream. From Eq. (1), we obtain

$$v=v_{0+}-\int_0^y(\partial u/\partial x)dy' \tag{7}$$

Substituting Eq. (7) into Eq. (2), integrating from $y=0$ to $y=\delta_1(x)$, where $\delta_1(x)$ is the boundary-layer thickness in the gas stream, we have

$$(U_1-u_{0+})v_{0+}-(\partial/\partial x)\int_0^{\delta_1}(U_1-u)u\,dy=-\nu_1(\partial u/\partial y)_{0+} \tag{8}$$

By assuming that u only depends on the similarity variable

$$\eta_1=y/\delta_1(x) \tag{9}$$

such that

$$(u/U_1)=\phi_1(\eta_1) \tag{10}$$

and that the mass blowing velocity v_{0+} varies inversely with $\delta_1(x)$,

$$v_{0+}=\nu_1\beta_1/\delta_1(x) \tag{11}$$

Eq. (8) becomes

$$(d/dx)[\delta_1(x)]^2=[(2\nu_1)/(U_1I_1)][\beta_1(1-\alpha)+\phi_1'(0)] \tag{12}$$

where

$$\alpha=u_{0+}/U_1 \quad I_1=\int_0^1(\phi_1-\phi_1^2)d\eta_1$$

and β_1 is an interfacial mass-transfer rate coefficient which is positive and negative for blowing and suction, respectively. Integrating Eq. (12) yields the boundary-layer thickness

$$[\delta_1(x)]^2=[(2\nu_1)/(U_1I_1)][\beta_1(1-\alpha)+\phi_1'(0)]x \tag{13}$$

Similarly, for the liquid stream, it can be shown that

$$[\delta_2(x)]^2=[(2\nu_2)/(U_1I_2)][\beta_2(\alpha-\lambda)+\phi_2'(0)]x \tag{14}$$

where

$$I_2=\int_0^1(\lambda\phi_2-\phi_2^2)d\eta_2 \qquad \eta_2=-y/\delta_2(x)$$

$$(u/U_1)=\phi_2(\eta_2) \qquad v_{0-}=\nu_2\beta_2/\delta_2(x)$$

and $\lambda=U_2/U_1$. Equations (13) and (14) show that the boundary-layer thicknesses vary with $x^{1/2}$, as would be expected. Furthermore, since the similar profiles for the streams both vary with $y/x^{1/2}$, the interfacial velocity $u(0)$ is found to be a constant.

Dividing Eq. (14) by Eq. (13), and noting that the interfacial relations Eqs. (5) and (6) can now be expressed as

$$\phi_1'(0)=-(\mu/\delta)\phi_2'(0) \qquad \beta_1=(\mu/\delta)\beta_2$$

the ratio of the boundary-layer thicknesses, $\delta=\delta_2(x)/\delta_1(x)$, is given by

$$\delta^2=\frac{1}{\rho}\frac{I_1}{I_2}\frac{[\beta_1(\alpha-\lambda)-\phi_1'(0)]}{[\beta_1(1-\alpha)+\phi_1'(0)]} \tag{15}$$

where $\mu=\mu_2/\mu_1$ and $\rho=\rho_2/\rho_1$.

To proceed further, the functional forms of $\phi_1(\eta_1)$ and $\phi_2(\eta_2)$ need to be specified. By assuming a polynomial representation and by requiring that the following relations

$$\phi_1(0)=\phi_2(0)=\alpha \qquad \phi_1(1)=1 \qquad \phi_2(1)=\lambda$$

$$\phi_1'(1)=\phi_2'(1)=0 \qquad \phi_1''(1)=\phi_2''(1)=0$$

$$\beta_1\phi_1'=\phi_1''(0) \qquad \beta_2\phi_2'(0)=-\phi_2''(0) \tag{16}$$

be satisfied, $\phi_1(\eta_1)$ and $\phi_2(\eta_2)$ are found to be

$$\phi_1(\eta_1)=\alpha+\frac{12(1-\alpha)}{(6+\beta_1)}[\eta_1+\tfrac{1}{2}\beta_1\eta_1^2-\tfrac{1}{3}(3+\beta_1)\eta_1^3+\tfrac{1}{4}(2+\beta_1)\eta_1^4] \tag{17}$$

$$\phi_2(\eta_2) = \alpha - \frac{12(\alpha-\lambda)}{(6-\beta_2)}\left[\eta_2 - \tfrac{1}{2}\beta_2\eta_2^2 - \tfrac{1}{3}(3-2\beta_2)\eta_2^3 + \tfrac{1}{4}(2-\beta_2)\eta_2^4\right] \quad (18)$$

The last two relations in Eq. (16) are obtained by evaluating Eqs. (2) and (3) at the interface. In the absence of interfacial mass transfer, as is the case treated by Lock,[7] $\phi_1''(0) = \phi_2''(0) = 0$ and the second degree terms, η_1^2 and η_2^2, vanish from Eqs. (17) and (18). This somewhat simplifies the subsequent derivation. However, in the presence of interfacial mass transfer these terms are essential since they allow for the possibility that the maximum shear may occur somewhere within the boundary layer removed from the interface.

Knowing $\phi_1(\eta_1)$ and $\phi_2(\eta_2)$, I_1 and I_2 can be evaluated, yielding

$$I_1 = \frac{(1-\alpha)}{35(6+\beta_1)^2}(5\alpha A_{11} + 4A_{12}) \quad (19)$$

$$I_2 = -\frac{(\alpha-\lambda)}{35(6-\beta_1\tau)^2}(5\alpha A_{21} + 4\lambda A_{22}) \quad (20)$$

where

$$A_{11} = 46 + 19\beta_1 + 2\beta_1^2, \quad A_{12} = 37 + 13\beta_1 + \beta_1^2$$

$$A_{21} = 46 - 19\beta_1\tau + 2(\beta_1\tau)^2, \quad A_{22} = 37 - 13\beta_1\tau + (\beta_1\tau)^2$$

and $\tau = \delta/\mu$.

Substituting I_1, I_2, and $\phi_1'(0)$ into Eq. (15), we finally obtain

$$\tau^2 = \frac{(6-\beta_1\tau)[12 - 6\beta_1\tau + (\beta_1\tau)^2][5\alpha A_{11} + 4A_{12}]}{\omega(6+\beta_1)[12 + 6\beta_1 + \beta_1^2][5\alpha A_{21} + 4\lambda A_{22}]} \quad (21)$$

where $\omega = \rho\mu$, and α is given by

$$\alpha = \frac{(6-\beta_1\tau)\tau + (6+\beta_1)\lambda}{(6-\beta_1\tau)\tau + (6+\beta_1)} \quad (22)$$

Hence by given mass transfer rate coefficient β_1, the ratio of the freestream velocities λ, and the density-viscosity ratio ω, the parameter τ can be determined iteratively from Eq. (21). Knowing τ, α is simply given by Eq. (22).

Blasius Analysis

Equations (1-3) can also be solved using the Blasius flat-plate analysis. The technique is standard[3,4,7,8] and yields

$$f_1'''(\tilde{\eta}_1) + f_1(\tilde{\eta}_1) f_1''(\tilde{\eta}_1) = 0 \quad (23)$$

$$f_2'''(\tilde{\eta}_2) + f_2(\tilde{\eta}_2) f_2''(\tilde{\eta}_2) = 0 \quad (24)$$

which are to be solved subject to the boundary conditions

$$f_1'(\infty) = 1, \quad f_2'(-\infty) = \lambda, \quad f_1'(0^+) = f_2'(0^-)$$

$$f_1(0^+) = \omega^{1/2} f_2(0^-), \quad f_1''(0^+) = \omega^{1/2} f_2''(0^-) \quad (25)$$

where

$$\tilde{\eta}_1 = [U_1/(2\nu_1 x)]^{1/2} y, \quad \tilde{\eta}_2 = [U_1/(2\nu_2 x)]^{1/2} y$$

and $f_1(0^+)$, which represents the mass-transfer rate, is given.

The normal mass flux in the present analysis is

$$\rho_1 v_{0+} = -(U_1\rho_1\mu_1/2x)^{1/2} f_1(0^+) \quad (26)$$

Comparing Eq. (11) with Eq. (26), it can be shown that the interfacial mass-transfer rate coefficients, β_1 and $f_1(0^+)$, for the two analyses are related through

$$f_1(0^+) = -\beta_1\left(\frac{5\alpha A_{11} + 4A_{12}}{35(6+\beta_1)(12 + 6\beta_1 + \beta_1^2)}\right) \quad (27)$$

A similar consideration for the interfacial shear yields a relation between β_1 and $f_1''(0^+)$

$$f_1''(0^+)/f_1(0^+) = -(12/\beta_1)(1-\alpha)/(6+\beta_1) \quad (28)$$

Using Eqs. (27) and (28), results from the two analyses can be compared directly.

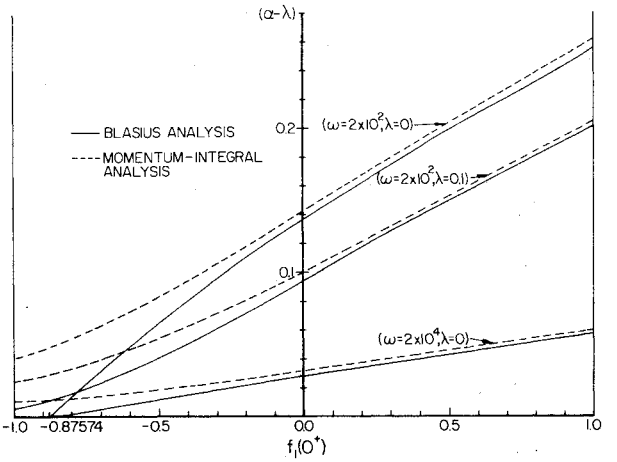

Fig. 1 Induced interfacial velocity $(\alpha-\lambda)$ as a function of the mass transfer rate coefficient $f_1(0^+)$, the ratio of the freestream velocities λ, and the density-viscosity ratio ω.

Results and Discussions

For given λ, ω, and β_1, Eq. (21) is solved by Newton-Ralphson's iteration method whereas Eqs. (23) and (24) are solved by quasilinearization and an implicit finite difference scheme. Figure 1 shows $(\alpha-\lambda)$ as a function of λ, ω, and $f_1(0^+)$. The values $\omega = 2\times10^4$ and 2×10^2 selected for study are respectively representative of situations where hydrocarbon droplets undergo combustion, in standard atmosphere and in a high-temperature, high-pressure environment typical within some internal combustion engines.

Figure 1 shows that the induced surface velocity $(\alpha-\lambda)$ decreases with increasing λ, increasing ω, and increasing amount of mass transfer into the gas stream. These effects are to be expected since higher values of ω imply the liquid is more viscous, hence less responsive to the interfacial shear; whereas mass addition into the gas stream thickens its boundary layer and subsequently reduces the interfacial shear.

Solutions from the momentum-integral analysis agree very satisfactorily with the more accurate Blasius analysis over the entire range of suction, although the agreement deteriorates at high blowing rates. In the Blasius analysis, for $\lambda = 0$, numerical convergence becomes increasingly difficult as $-f_1(0^+)$ increases; hence values of $-f_1(0^+)$ above 0.85 are extrapolated. However, $(\alpha-\lambda)$ seems to approach zero at the classical limit $-f_1(0^+) = 0.87574$ for rigid flat-plates,[8,9] where the blowing is at such a high rate that the gas-phase boundary layer becomes infinitely thick and the interfacial shear vanishes. The momentum-integral analysis fails to predict this critical state.

It can be concluded that the simplified solutions of the momentum-integral analysis are quite accurate in predicting the integrated characteristics of two dissimilar, parallel streams with interfacial mass transfer over the entire range of suction and also for moderate blowing rates.

References

[1] Law, C. K., "Unsteady Droplet Combustion with Droplet Heating," *Combustion and Flame*, Vol. 26, 1976, pp. 17-22.

[2]Law, C. K., "Multicomponent Droplet Combustion with Rapid Internal Mixing," *Combustion and Flame*, Vol. 26, 1976, pp. 219-233.

[3]Law, C. K. and Sirignano, W. A., "Flat-Plate Combustion of Multicomponent Liquid Fuels," Paper No. 4, 1975 Fall Technical Meeting of the Eastern States Section of the Combustion Institute, Oct., 1975.

[4]Law, C. K., Prakash, S., and Sirignano, W. A., "Theory of Convective, Transient, Multicomponent Droplet Vaporization," presented at the Sixteenth International Symposium on Combustion, Cambridge, Mass., 1976.

[5]Landis, R. B. and Mills, A. F., "Effects of Internal Diffusional Resistance on the Evaporation of Binary Droplets," Paper B7.9, 5th International Heat Transfer Conference, Tokyo, 1974.

[6]El Wakil, M. M., Priem, R. J., Brikowski, H. J., Myers, P. S., and Uyehara, O. A., "Experimental and Calculated Temperature and Mass Histories of Vaporizing Fuel Droplets," NASA TN-3490, 1956.

[7]Lock, R. C., "The Velocity Distribution in the Laminar Boundary Layer Between Parallel Streams," *Quarterly Journal of Mechanics and Applied Mathematics*, Vol. IV, 1951, pp. 42-57.

[8]Emmons, H. W., "The Film Combustion of Liquid Fuel," *Zeitschrift Fuer Angewandte Mathematik Und Mechanik*, Vol. 36, 1956, pp. 60-71.

[9]Kassoy, D. R., "Similar Laminar Boundary Layers with Zero Wall Shear and Mass Addition," *AIAA Journal*, Vol. 9, April 1971, pp. 725-728.

Comparison of Conventional and Force-Based Distortion Index Measurements

M. Sajben,* C.P. Chen,† and J.C. Kroutil†
McDonnell Douglas Corporation, St. Louis, Mo.

STEADY flow nonuniformities at the diffuser/compressor interface of airbreathing inlets significantly influence the surge behavior of jet engines. The proper characterization of such distortions is recognized to have an important bearing on both inlet and compressor design.[1,2] Many definitions of descriptive indices have been proposed, but few have gained wide acceptance.

In a recent paper,[3] the suggestion was made that an indicator of velocity nonuniformity can be deduced from the measurement of force associated with the integrated impulse $(p+\rho u^2)$. Strong theoretical and practical reasons favor such an index,[3] one of which is that it correlates well with one of the most widely accepted indicators of distortion, and valid comparisons therefore can be made with existing data presented in terms of other types of indices. Experiments supporting this claim are described in this note.

The distortion index proposed here relies on force and flow rate measurements that are made routinely in thrust stands to determine nozzle flow and thrust coefficients. If the experiment is arranged appropriately,[3] the index can be computed as

$$\psi_x = \bar{\rho} A F_x / \dot{m}^2 \tag{1}$$

where $\bar{\rho}$ is the area-averaged density, A is the exit area (assumed plane and normal to the x axis), $\dot{m}$ is the mass flow and F_x is the x component of the force corresponding to the impulse integrated over A.

Received Oct. 29, 1975; revision received May 24, 1976. This research was conducted under the McDonnell Douglas Independent Research and Development program.

Index categories: Nozzle and Channel Flow; Airbreathing Propulsion, Subsonic and Supersonic.

*Senior Scientist, Research Laboratories. Associate Fellow AIAA.

†Research Scientist, Research Laboratories.

The integral of the impulse contains a contribution from the static pressure. The test usually can be arranged such that this contribution is small; the following approximate equality is then valid

$$\psi_x - 1 \cong \frac{1}{\rho \bar{u}^2 A} \int_A \rho (u-\bar{u})^2 dA \tag{2}$$

Equation (2) shows that $(\psi_x - 1)$ is zero for uniform flows and is increasingly greater than zero as the velocity distribution becomes more nonuniform. The index is appropriate for preliminary, configuration screening studies. More complex indices, reflecting radial and circumferential dependencies, are used for detailed inlet evaluations.

The proposed index offers both theoretical and practical benefits. Its definition is rigorously compatible with the momentum equation and therefore is well suited to complement theoretical calculation, especially integral methods. The required measurements are routine on conventional thrust stands. Flowfield details need not be determined, eliminating problems of flow obstruction by probe rakes. The number of transducers is reduced greatly, simplifying both calibration and data recording procedures. The measurement is insensitive to flowfield complexities such as intense turbulence or separation which generally prevent a reliable interpretation of signals from conventional total pressure probes.

Definitions of conventional indices do not permit derivation of theoretical correlations with ψ_x. To determine the empirical correlation, a test series was conducted in which three different indices were measured simultaneously.

Two conventional indices were chosen for comparison with ψ_x, both of which require total pressure measurements at 48 positions over the exit plane, in a manner customary in inlet testing. The first index, designated as ζ, is defined as

$$\zeta = (p_{t,\max} - p_{t,\min})/\bar{p}_t \tag{3}$$

where $p_{t,\max}$ ($p_{t,\min}$) is the maximum (minimum) indicated total pressure from the set of 48 and $\bar{p}_t$ is the area average of all readings. All pressures are time-averaged values.

ζ measures nonuniformity in terms of total pressure whereas ψ_x is defined in terms of velocity, resulting in different types of dependence on the (cross-sectional averaged) Mach number. For low and moderate Mach numbers ($M<0.3$), the relationship between the two indices is described approximately by the following relation

$$\zeta/\bar{M}^2 \cong C\left[(u^2_{\max} - u^2_{\min})/\bar{u}^2\right] \tag{4}$$

where C is a constant and $\bar{M}$ and $\bar{u}$ are averages of Mach number and axial velocity over the exit cross section, respectively. The bracket in Eq. (4) depends on the normalized velocity distribution, as does ψ_x. It follows that the quantity to be compared with ψ_x is not ζ but the ratio $\zeta/\bar{M}^2$.

A second index chosen for comparison, one of the most complex indices currently in use, is defined (in the notation of Ref. 4) as

$$K_{a2} = K_\theta + bK_{ra2} \tag{5}$$

where K_θ characterizes the circumferential and K_{ra2} the radial nonuniformities. The coefficient b is a weighting factor, dependent on the engine type. Details of the rather complex definitions can be found in Ref. 4. Data appropriate to the Pratt & Whitney F-100-FW-100 engine were used. The normalization employed in computing K_{a2} is such that K_{a2} is directly comparable with ψ_x. (Division by $\bar{M}^2$ is not necessary, as in the case with ζ.)

The measurements were conducted using seven different, axisymmetric diffusers, whose dimensions are given in Table 1. Reynolds number based on throat diameter ranged from 0.3×10^6 to 1.3×10^6. Throat Mach numbers ranged from 0.15 to 0.6. The flow exhausted to the atmosphere. No hub was employed at the diffuser exit, and an additional (49th) total pressure probe was located on the axis. The